Physics and Imaging in Radiation Oncology 14 (2020) 39–42

Contents lists available at ScienceDirect

Physics and Imaging in Radiation Oncology

journal homepage: www.elsevier.com/locate/phro

Technical Note

Accurate estimation of daily delivered radiotherapy dose with an external treatment planning system

Takahiro Kanehira[a], Stina Svensson[b], Simon van Kranen[a], Jan-Jakob Sonke[a,*]

[a] Department of Radiation Oncology, The Netherlands Cancer Institute, 1066 CX Amsterdam, The Netherlands
[b] RaySearch Laboratories AB, Stockholm, Sweden

ARTICLE INFO

Keywords:
Dose recalculation
Multi-institutional collaboration
Dose mimicking
Treatment planning system

ABSTRACT

Accurate estimation of the daily radiotherapy dose is challenging in a multi-institutional collaboration when the institution specific treatment planning system (TPS) is not available. We developed and evaluated a method to tackle this problem. Residual errors in daily estimations were minimized with single correction based on the planned dose. For nine patients, medians of the absolute estimation errors for targets and OARs were less than 0.2 Gy (D_{mean}), 0.3 Gy (D_1), and 0.1 Gy (D_{99}). In general, mimicking errors were significantly smaller than dose differences caused by anatomical changes. The demonstrated accuracy may facilitate dose accumulation in a multi-institutional/multi-vendor setting.

1. Introduction

Anatomical changes over the course of radiotherapy may induce differences between planned and delivered dose [1–3]. Early detection of such discrepancies may facilitate effective adaptive interventions [4], while dose effect relations on delivered dose may improve toxicity modeling [5]. Daily images, acquired routinely for Image Guided Radiotherapy (IGRT), can serve as basis for dose recalculations to estimate the daily delivered dose. Most studies that include daily recalculated dose are limited to a single institute with a single vendor treatment planning system (TPS) for dose recalculations [6–8]. To extend the use of daily delivered dose in multi-institutional studies with multiple-vendor TPSs, such as the ARTFORCE study [9], is challenging since plans are often not exchangeable between TPSs, dose models may differ, and institution machine specifics are unknown.

To overcome these challenges, we propose a new method to estimate daily delivered dose by using an external TPS that can optimize a new treatment plan to deliver the same dose distribution as the planned from the institutional TPS. Residual errors in daily estimations are minimized with a single correction based on the planned dose. In this technical note, we explore this method for nine head and neck cancer (HNC) patients.

2. Materials and methods

2.1. Patient/treatment data

Nine HNC patients, treated in the Antoni van Leeuwenhoek hospital, with considerable anatomy changes during treatment were retrospectively selected (Supplementary Table 1 for dose distribution abbreviations). Institutional review board approval was obtained. All patients had received non-adaptive radiotherapy with an Elekta Synergy linac (Elekta Oncology Systems Ltd., Crawley, West Sussex, UK). All patients received a planning CT (pCT) scan (3 mm slice thickness) on which targets and organs-at-risk (OARs) were contoured. Volumetric modulated arc therapy plans with simultaneous integrated boost were generated using the TPS Pinnacle (version 9.10, Philips Radiation Oncology Systems, Fitchburg, WI), which we call institutional TPS (TPS_I) for the rest of this note. Planned dose is denoted as $D_{TPS,0}$. Dose calculation grid size was 3 mm isotropically. High risk planning target volume (PTV_1) and elective (PTV_2) were prescribed to receive 70 Gy and 54.25 Gy in 35 fractions. Daily cone-beam computed tomography (CBCT) scans, with a field of view (FOV) of 40 cm × 40 cm × 25 cm, were acquired for all the patients prior to irradiation for online setup correction by multi-clipbox registration [10].

2.2. Mimic-plans

The RayStation TPS (version 5, RaySearch Laboratories AB,

* Corresponding author.
E-mail address: j.sonke@nki.nl (J.-J. Sonke).

https://doi.org/10.1016/j.phro.2020.05.005
Received 30 December 2019; Received in revised form 16 May 2020; Accepted 18 May 2020

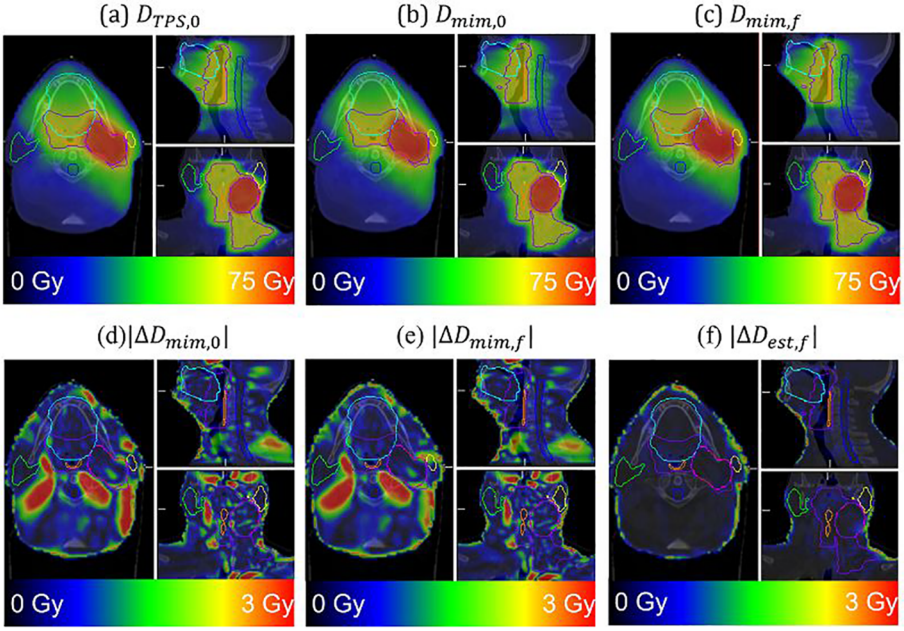

Fig. 1. Distributions of (a) planned dose, $D_{TPS,0}$, (b) mimic dose, $D_{mim,0}$, (c) mimic dose during treatment, $D_{mim,f}$, (d) absolute mimic dose error in the planning CT, $|\Delta D_{mim,0}|$, (e) during treatment without correction, $|\Delta D_{mim,f}|$ and f) during treatment with correction, $|\Delta D_{est,f}|$ ($D_{est,f} = D_{mim,f} - \Delta D_{mim,0}$).

Stockholm, Sweden), which we call mimicking TPS (TPS_M) for the rest of this note, can automatically generate mimic-plans of other treatment plans using a dose mimicking algorithm [11,12]. In this study, mimic-plans were generated by mimicking the planned dose as created by TPS_I. First, the pCT, treatment plan, planned dose distribution, and structure sets, originally generated with TPS_I were imported in TPS_M. Next, we selected a template treatment machine from a library, which best resembled (e.g. Elekta Synergy, 6MV) the one actually used for patient treatment. Mimic-plans were optimized by minimizing a cost function on differences in mean/maximum/minimum dose between planned dose and mimic-dose ($D_{mimic,0}$) for targets, OARs, and an external contour. Weighting factors ranking the importance of dosimetric parameters were all set to one. The dose calculation grid size was 3 mm isotropically.

2.3. Dose recalculation

Since CBCT Hounsfield Units and associated dose calculation accuracy are limited [13], a simulated daily CT (sCT) was generated independent from TPS_M as follows [14]: 1) deformable image registration (DIR) deformed CBCT onto pCT (after setup correction) using an in-house B-spline based algorithm [15,16], 2) sCT was created with an inverse of the DIR deforming the pCT onto the CBCT. For outside of CBCT's FOV, the rigid component of the DIR was used to patch the pCT. Daily dose at f^{th} fraction was estimated by recalculating the treatment plan on the sCT with the TPS_I ($D_{TPS,f}$). This daily dose was used as a gold standard for evaluating daily dose estimated by methods proposed in Section 2.4. As the largest anatomical changes typically occur at the end of treatment, we only evaluated dose at the last fraction for this study.

2.4. Method to estimate daily dose

A schematic representation of an estimation method for the delivered dose with TPS_M is shown in Supplementary Fig. 1. Our goal was to estimate $D_{TPS,f}$ using $D_{TPS,0}$, $D_{mim,0}$, and $D_{mim,0}$ recalculated on the sCT in TPS_M ($D_{mim,f}$). As the mimic-plan was not an exact copy of the original plan, the mimicked dose included mimic-errors (e. g. in the pCT: $\Delta D_{mim,0} = D_{mim,0} - D_{TPS,0}$), which propagated to errors in $D_{mim,f}$ (e. g. in the sCT: $\Delta D_{mim,f} = D_{mim,f} - D_{TPS,f}$). Therefore, to reduce mimic-errors, daily dose was estimated by calculating: $D_{est,f} = D_{mim,f} - \Delta D_{mim,0}$. $\Delta D_{mim,0}$ works as corrections for mimic-errors on the assumption that mimic-errors in the sCT is approximated by those in the pCT: $\Delta D_{mim,f} \sim \Delta D_{mim,0}$. Note that $\Delta D_{mim,0}$ was applied in the daily CT reference field without deformations although these dose distributions were not calculated on the same anatomy. The rationale behind this approach was the observation that mimic-errors were mostly associated with the machine coordinate system (e.g. MLC positions) rather than the patient coordinate system. For dosimetric evaluation, dose distributions were mapped on the pCT using the DIRs obtained in Section 2.3.

2.5. Dosimetric evaluations

Accuracy of $D_{mim,0}$ was compared to that of $D_{TPS,0}$ for absolute errors in dosimetric parameters ($D_{mean}/D_1/D_{99}$) for regions of interest (ROIs): PTV_1, PTV_2, ipsilateral/contralateral parotid gland (IPG/CPG), constrictor muscle (CM), oral cavity (OC), and spinal cord (SC). We evaluated the dosimetric accuracy of $D_{est,f}$ and $D_{mim,f}$ compared to $D_{TPS,f}$ regarding absolute errors in the dosimetric parameters, voxel-by-voxel absolute dose errors (DE), and dose volume histogram (DVH) curves. Additionally, the absolute estimation errors were compared to dose differences (DDs) induced by anatomical changes calculated as absolute differences in the parameters between $D_{TPS,f}$ and $D_{TPS,0}$. Wilcoxon signed-rank tests were performed to 1) compare the absolute estimation errors with the absolute DDs induced by anatomical changes and 2) compare the absolute estimation errors of $D_{est,f}$ with those of $D_{mim,f}$ using SciPy (version 0.19.1) (statistical significance of p-value < 0.05 with multiple tests correction of Benjamini-Hochberg procedure). All dosimetric evaluations were performed in the pCT using DIRs employed to deform CBCT onto pCT.

3. Results

3.1. Mimic-plan

Mimic-plan accuracy was evaluated with the absolute differences between planned dose and mimic-dose. DEs in mimic-dose larger than

3 Gy were more pronounced in the regions not included in the optimization objectives than in the ROIs (Fig. 1(d)). Additionally, differences in dosimetric parameters between planned dose and mimic-dose for the ROIs for the nine patients were assessed (Supplementary Fig. 2). The medians of the errors in the dosimetric parameters for ROIs were less than 0.6 Gy (D_{mean}), 0.8 Gy (D_1), and 2.7 Gy (D_{99}).

3.2. Estimated daily dose accuracy

$D_{mim,f}$ and $D_{est,f}$ were evaluated compared to $D_{TPS,f}$. The error distribution of $D_{mim,f}$ in daily CT was similar to the dose mimicking error distribution in the pCT (Fig. 1(d-e)). In contrast, error of $D_{est,f}$ ($\Delta D_{est,f} = D_{est,f} - D_{TPS,f}$) was small over the whole scan (Fig. 1.(f)). The DVH curves for $D_{est,f}$ were closer to the gold standard ($D_{TPS,f}$) than those for $D_{mim,f}$(Supplementary Fig. 3). Regarding voxel-by-voxel accuracy, the percentage of the voxels with DEs for $D_{est,f}$ < 2% of the prescribed dose was > 98% for targets/OARs, and 95% for the volume planned to receive > 50% of the prescribed dose to PTV_2 ($V_{50\%}$). Without correction, $D_{min,f}$, these percentages were > 74% (targets/OARs) and 64.9% ($V_{50\%}$) (Supplementary Fig. 4).

$D_{mim,f}$ and $D_{est,f}$ were also evaluated on dosimetric parameters for the ROIs. The medians of the discrepancies were less than 0.2 Gy (D_{mean}), 0.3 Gy (D_1), and 0.1 Gy (D_{99}) for $D_{est,f}$ whereas they were less than 0.6 Gy, 0.6 Gy, and 1.9 Gy for $D_{mim,f}$ (Fig. 1, Supplementary Table 2). The discrepancies for $D_{est,f}$ were significantly smaller than those for $D_{mim,f}$ (11/21 ROIs)(p-value < 0.05) (Supplementary Table 4). Furthermore, we compared the mimicking errors with differences arising from anatomical changes (Fig. 2). For a large majority of the dosimetric parameters (15/21 ROIs), the errors for $D_{est,f}$ were significantly smaller (p-value < 0.05) than the DDs induced by anatomical changes (ΔD_{mean} from 1.0 Gy to 4.3 Gy), indicating that the detection threshold was sufficient to find significant DDs induced by anatomy changes in 15/21 ROIs. Without correction, i.e., in $D_{min,f}$, sensitivity was only sufficient to find true DDs in 10/21 ROIs (Supplementary Table 4).

4. Discussion

We developed a novel method to estimate daily dose with a TPS that can mimic treatment plans from other TPSs. The method was evaluated for estimating delivered dose in the last fraction for nine HNC patients and for a single combination of TPS and treatment machine. The proposed method demonstrated accurate dosimetric estimation of the impact of anatomical changes.

In line with previous studies, we found that mimic-plans were not exact copies of original plans and exhibited errors in mimic-doses [11,12]. To improve the accuracy of dose estimations in daily scans, we introduced a correction derived from the mimic planned dose ($\Delta D_{mim,0} = D_{mim,0} - D_{TPS,0}$). As a result, the median errors were less than 0.2 Gy (D_{mean}), 0.3 Gy (D_1), and 0.1 Gy (D_{99}) for targets/OARs. A systematic review on changes in OAR dose in HNC patients showed typical change in PG D_{mean} of > 2 Gy [17] while a dose accumulation study in our institute showed OAR D_{mean} changes from 0.4 Gy (SC) to 1.2 Gy (IPG) [6]. This suggests that our method can be used to estimate daily doses accurate enough to observe relevant dose changes during treatments. Furthermore, our method can be potentially applied for dose accumulation, where voxels receiving significant dose should be accurately aligned [18]. The voxel-by-voxel DEs were smaller than typical dose accumulation uncertainties (91% of voxels within 2% DDs among different DIRs [19] and 90% of voxels within 2% DE when sCT replaced rCT [20]).

Regarding mimic-plan accuracy, relatively small DEs were found in the ROIs while larger errors were found in undefined regions. Secondly, due to the design of the cost-function for optimizing the mimic-plan (constraints on mean/min/max DDs with planned), discrepancies may arise in large volumes. Here the driving force is determined by large min/max DEs (single voxels) while substantial subvolumes with hot/cold spots can remain because they cancel out in the mean DEs. The mimicking dose objectives were empirically selected but a further refinement could be possible. An alternative to dose mimicking would be to import the treatment plan and recalculate the dose using general template machine parameters. Due to differences between TPSs in how

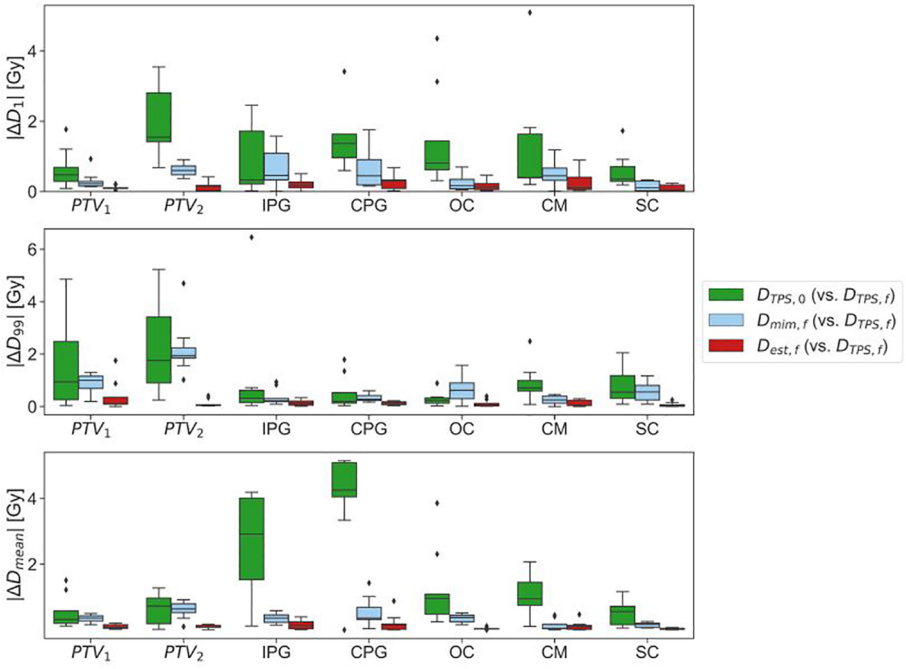

Fig. 2. Boxplots of absolute errors in dosimetric parameters for $D_{mim,f}$ (light blue) and $D_{est,f}$ (red) and absolute differences in the parameters caused by anatomical changes ($D_{TPS,0}$ vs. $D_{TPS,f}$) (green) for high risk planning target volume (PTV_1) and elective (PTV_2), ipsilateral and contralateral parotid gland (IPG and CPG), constrictor muscle (CM), oral cavity (OC), and spinal cord (SC) for nine patients. A few outliers are not shown in the graphs for visualization purpose. (For interpretation of the references to colour in this figure legend, the reader is referred to the web version of this article.)

they handle machine constraints, only a subset of plans would be eligible for such an approach and differences can be larger without an effort to minimize differences between the original and recalculated dose distribution.

Ground truth dose calculations were made with a sCT, deformed from CBCT, which may not accurately represent the CBCT anatomy due to the DIR inaccuracy. As a result, DDs may arise compared to direct (ideal) CBCT dose calculations. However, the sCT could have been replaced with a repeat CT (rCT), without anatomy errors, with little consequences for the presented results since the comparison was made between calculated dose with and without correction. Our purpose was not to obtain the best CBCT-based dose calculation, but to evaluate the performances of mimic-plans plus correction. In fact, using the DIR to both create a sCT and map the recalculated dose back to the pCT inherently leads to a consistent mapping of the dose without errors, better than can be expected from a rCT plus DIR.

There are several limitations in this study. First, only HNC patients were evaluated, requiring further evaluations for other tumor sites. Second, only a single combination of institutional and external TPS, and treatment machine, was evaluated. Whether the proposed approach extends new TPS and other machines needs to be evaluated. Finally, the number of patients was small, so caution is warranted before drawing definitive conclusions.

A future application of the presented method is dose accumulation in multi-institutional collaborations where a single institution with a DA infrastructure estimates daily doses and accumulate the doses over fractions for other institutions' patients. This is useful because a dose accumulation infrastructure is not currently clinical routine in many institutions.

In conclusion, we have developed a method to accurately estimate daily dose with a TPS that supports plan mimicking. By applying a correction to account for residual DEs, we found that the accuracy was sufficient to observe relevant dose changes during HNC radiotherapy.

Funding statement

This research was partially funded by Health Holland public-private partnership grant (LSHM15036) in collaboration with Elekta Oncology Systems AB.

Declaration of Competing Interest

The authors declare the following financial interests/personal relationships which may be considered as potential competing interests: The department of radiation oncology of the Netherlands Cancer Institute receives license fees from Elekta Systems AB, Sweden for Cone Beam CT guided software. Stina Svensson is an employee of a vendor (RaySearch Laboratories AB, Stockholm, Sweden) for treatment planning system RayStation.

Appendix A. Supplementary data

Supplementary data to this article can be found online at https://doi.org/10.1016/j.phro.2020.05.005.

References

[1] Ahn P, Chen C, Ahn A, Scripes P, Shen J, Lee C, et al. Adaptive planning in intensity-modulated radiation therapy for head and neck cancers: single-institution experience and clinical implications. Int J Radiat Oncol Biol Phys 2011;80:677–85. https://doi.org/10.1016/j.ijrobp.2010.03.014.

[2] Broggi S, Fiorino C, Dell I, Dinapoli N, Paiusco M, Muraglia A, et al. A two-variable linear model of parotid shrinkage during IMRT for head and neck cancer. Radiother Oncol 2010;94:206–12. https://doi.org/10.1016/j.radonc.2009.12.014.

[3] Vásquez Osorio E, Hoogeman M, Al-Mamgani A, Teguh D, Levendag P, Heijmen B. Local anatomic changes in parotid and submandibular glands during radiotherapy for oropharynx cancer and correlation with dose, studied in detail with nonrigid registration. Int J Radiat Oncol Biol Phys 2008;70:875–82. https://doi.org/10.1016/j.ijrobp.2007.10.063.

[4] Heukelom J, Kantor ME, Mohamed ASR, Elhalawani H, Kocak-uzel E, Lin T, et al. Differences between planned and delivered dose for head and neck cancer, and their consequences for normal tissue complication probability and treatment adaptation. Radiother Oncol 2020;142:P100–6. https://doi.org/10.1016/j.radonc.2019.07.034.

[5] Shelley LEA, Scaife JE, Romanchikova M, Harrison K, Forman JR, Bates AM, et al. Delivered dose can be a better predictor of rectal toxicity than planned dose in prostate radiotherapy. Radiother Oncol 2017;123:466–71. https://doi.org/10.1016/j.radonc.2017.04.008.

[6] Van Kranen S, Hamming-vrieze O, Van Herk M, Wolf A, Sonke JJ. Head and neck margin reduction with adaptive radiation therapy: robustness of treatment plans against anatomy changes. Int J Radiat Oncol Biol Phys 2016;96:653–60. https://doi.org/10.1016/j.ijrobp.2016.07.011.

[7] Lou J, Huang P, Ma C, Zheng Y, Chen J, Liang Y, et al. Parotid gland radiation dose-xerostomia relationships based on actual delivered dose for nasopharyngeal carcinoma. J Appl Clin Med Phys 2018;19:251–60. https://doi.org/10.1002/acm2.12327.

[8] Thor M, Andersen ES, Petersen JBB, Sørensen TS, Noe KØ, Tanderup K, et al. Evaluation of an application for intensity-based deformable image registration and dose accumulation in radiotherapy. Acta Oncol 2014;53:1329–36. https://doi.org/10.3109/0284186X.2014.928742.

[9] Heukelom J, Hamming O, Bartelink H, Hoebers F, Giralt J, Herlestam T, et al. Adaptive and innovative Radiation Treatment FOR improving Cancer treatment outcomE (ARTFORCE); a randomized controlled phase II trial for individualized treatment of head and neck cancer. BMC Cancer 2013;13:84. https://doi.org/10.1186/1471-2407-13-84.

[10] Van Beek S, Van Kranen S, Mencarelli A, Remeijer P, Rasch C, van Herk M, et al. First clinical experience with a multiple region of interest registration and correction method in radiotherapy of head-and-neck cancer patients. Radiother Oncol 2010;94:213–7. https://doi.org/10.1016/j.radonc.2009.12.017.

[11] Zhang X, Penagaricano J, Narayanasamy G, Corry P, Liu TX, Sanjay M, et al. Helical tomotherapy to LINAC plan conversion utilizing RayStation Fallback planning. J Appl Clin Med Phys 2017;18:178–85. https://doi.org/10.1002/acm2.12032.

[12] Petersson K, Nilsson P, Engström P, Knöös T. Evaluation of dual-arc VMAT radiotherapy treatment plans automatically generated via dose mimicking generated via dose mimicking. Acta Oncol 2016;55:523–5. https://doi.org/10.3109/0284186X.2015.1080855.

[13] Hatton J, McCurdy B, Greer PB. Cone beam computerized tomography: the effect of calibration of the Hounsfield unit number to electron density on dose calculation accuracy for adaptive radiation therapy. Phys Med Biol 2009;54:N329–46. https://doi.org/10.1088/0031-9155/54/15/N01.

[14] Peroni M, Ciardo D, Spadea F, Riboldi M, Comi S, Alterio D, et al. Automatic segmentation and online virtual CT in head-and-neck adaptive radiation therapy. Radiat Oncol Biol 2012;84:e427–33. https://doi.org/10.1016/j.ijrobp.2012.04.003.

[15] Van Kranen S, Mencarelli A, Van Beek S, Rasch C, Van Herk M, Sonke JJ. Adaptive radiotherapy with an average anatomy model: evaluation and quantification of residual deformations in head and neck cancer patients. Radiother Oncol 2013;109:463–8. https://doi.org/10.1016/j.radonc.2013.08.007.

[16] Mencarelli A, van Kranen SR, Hamming-vrieze O, van Beek S, Rasch CR, van herk M, Sonke JJ. Deformable image registration for adaptive radiation therapy of head and neck cancer: accuracy and precision in the presence of tumor changes. Radiat Oncol Biol 2014;90:680–7. https://doi.org/10.1016/j.ijrobp.2014.06.045.

[17] Brouwer CL, Steenbakkers RJHM, Langendijk JA, Sijtsema NM. Identifying patients who may benefit from adaptive radiotherapy: does the literature on anatomic and dosimetric changes in head and neck organs at risk during radiotherapy provide information to help? Radiother Oncol 2015;115:285–94. https://doi.org/10.1016/j.radonc.2015.05.018.

[18] Brock KK, Mutic S, Mcnutt TR, Li H, Kessler ML. Use of image registration and fusion algorithms and techniques in radiotherapy: report of the AAPM Radiation Therapy Committee Task Group No. 132. Med Phys 2017;44:e43–76. https://doi.org/10.1002/mp.12256.

[19] Veiga C, Lourenco A, Mouinuddin S, Van Herk M, Modat M, Ourselin S, et al. Toward adaptive radiotherapy for head and neck patients: uncertainties in dose warping due to the choice of deformable registration algorithm. Med Phys 2015;42:760–9. https://doi.org/10.1118/1.4905050.

[20] Veiga C, Mcclelland J, Moinuddin S, Lourenço A, Ricketts K, Annkah J, et al. Toward adaptive radiotherapy for head and neck patients: feasibility study on using CT-to-CBCT deformable registration for "dose of the day" calculations. Med Phys 2014;41:1–12. https://doi.org/10.1118/1.4864240.